

## Monomeric $\alpha$ -synuclein ( $\alpha$ S) inhibits amyloidogenesis of human prion protein (hPrP) by forming a stable $\alpha$ S-hPrP hetero-dimer.

Satoshi Yamashita<sup>a</sup>, Yuji O. Kamatari<sup>a,b</sup>, Ryo Honda <sup>a</sup>, Ayumi Niwa<sup>c</sup>, Hiroyuki Tomiata<sup>c</sup>, Akira Hara<sup>c</sup>, and Kazuo Kuwata<sup>a,d</sup>

<sup>a</sup>United Graduate School of Drug Discovery and Medical Information Sciences, Gifu University, Tokai National Higher Education and Research System, Gifu, Japan; <sup>b</sup>Institute for Glyco-core Research, Tokai National Higher Education and Research System, Gifu, Japan; <sup>c</sup>Department of Tumor Pathology, Gifu University Graduate School of Medicine, Tokai National Higher Education System, Gifu, Japan; <sup>d</sup>Department of Gene and Development, Gifu University School of Medicine, Tokai National Higher Education and Research System, Gifu, Japan

### ABSTRACT

Intermolecular interaction between hPrP and  $\alpha$ S was investigated using high-speed atomic force microscopy, dynamic light scattering, and nuclear magnetic resonance. We found that hPrP spontaneously gathered and naturally formed oligomers. Upon addition of monomer  $\alpha$ S with a disordered conformation, poly-dispersive property of hPrP was lost, and hetero-dimer formation started quite coherently, and further oligomerization was not observed. Solution structure of hPrP- $\alpha$ S dimer was firstly characterized using hetero-nuclear NMR spectroscopy. In this hetero-dimeric complex, C-terminal helical region of hPrP was in the molten-globule like state, while specific sites including hot spot and C-terminal region of  $\alpha$ S selectively interacted with hPrP. Thus  $\alpha$ S may suppress amyloidogenesis of hPrP by trapping the hPrP intermediate by the formation of a stable hetero-dimer with hPrP.

**Abbreviations:** hPrP, human prion protein of amino acid residues of 23-231; PrP<sup>C</sup>, cellular form of prion protein; PrP<sup>Sc</sup>, scrapie form of prion protein, HS-AFM; high speed atomic force microscopy;  $\alpha$ S,  $\alpha$ -synuclein; DLS, dynamic light scattering

### ARTICLE HISTORY

Received 13 January 2021

Revised 3 March 2021

Accepted 24 March 2021

### KEYWORDS

$\alpha$ -synuclein; prion; hetero-oligomer; pathogenic conversion; AFM

### Introduction

Intermolecular interaction is a key pathological event in protein misfolding disease [1,2]. Amyloid deposits are mainly composed of a specific disease-associated amyloidogenic protein, such as amyloid- $\beta$  (A $\beta$ ) in Alzheimer's disease [3],  $\alpha$ -synuclein ( $\alpha$ S) in Parkinson's disease [4], and prion protein (PrP) in transmissible spongiform encephalopathy [5]. Recent evidence has indicated that several amyloidogenic proteins can interact with a different disease-associated protein to dramatically impact on the development of amyloid deposits [6]. Cross-seeding is also a prominent example of the cross-interactions, by which an amyloid fibril composed of one specific protein can promote amyloidogenesis of a different amyloidogenic protein [7].

On the other hand, specific interactions between amyloidogenic proteins were reported. Lauren et al [8], suggested that cellular prion protein (PrP<sup>C</sup>) on cell surface serves as a receptor for oligomeric amyloid  $\beta$ (A $\beta$ ) and blocks the long term potentiation (LTP) upon A $\beta$  binding, although it was reported later that

A $\beta$ 42 blocks LTP even without PrP<sup>C</sup> [9]. Selective inhibition of amyloidogenic proteins against amyloidogenesis was also reported, such as chaperone-like activity of  $\alpha$ -synuclein ( $\alpha$ S) [10–14], which may lead to the development of therapeutics.

We previously confirmed that monomeric  $\alpha$ S suppressed amyloid formation of human prion protein (hPrP) [14]. Although  $\alpha$ -synuclein ( $\alpha$ S) amyloids reportedly interacts with hPrP and blocks prion replication [15], in our experiment A $\beta$  amyloid was strongly bound with hPrP but  $\alpha$ S amyloid [15]. However, structural evidence of the direct interaction between monomeric  $\alpha$ S and hPrP was still elusive.

The present study aimed to characterize the intermolecular interaction between hPrP and monomeric  $\alpha$ S in molecular shape resolution as well as in atomic resolution. To do this, we initially applied high-speed atomic force microscopy (HS-AFM) [16] for the observation of the real-time molecular shape alteration of hPrP and  $\alpha$ S upon mixing. HS-AFM was useful for the observation of protein aggregation process [17], particularly for the real-time observation as presented here.

**CONTACT** Kazuo Kuwata  [Kuwata@gifu-u.ac.jp](mailto:Kuwata@gifu-u.ac.jp)  United Graduate School of Drug Discovery and Medical Information Sciences, Gifu University, Tokai National Higher Education and Research System, Gifu 501-1193, Japan

 Supplemental data for this article can be accessed [here](#).

© 2021 The Author(s). Published by Informa UK Limited, trading as Taylor & Francis Group.

This is an Open Access article distributed under the terms of the Creative Commons Attribution License (<http://creativecommons.org/licenses/by/4.0/>), which permits unrestricted use, distribution, and reproduction in any medium, provided the original work is properly cited.

We then measured dynamic light scattering (DLS) [18,19] for resolving the population of conformers in a mixture of hPrP and  $\alpha$ S. Finally, we measured various  $^1\text{H}$ - $^{15}\text{N}$  HSQC spectra to elucidate the conformational characteristics of the hPrP- $\alpha$ S complex, and discussed the possible inhibitory mechanism of  $\alpha$ S upon hPrP pathogenic conversion reaction.

## Results

### Dispersive oligomer configurations of hPrP

HS-AFM imaging of hPrP at a concentration of 30 nM revealed that particle diameters of hPrP were distributed from 2 nm to 100 nm corresponding to monomer to various sizes of oligomers, and generally consisted of a head and tail (Figure 1a). Height analysis of a large oligomer (Figure 1b) revealed that the diameter of its body was around 8 nm and its tail was 2 nm.

According to AFM calibration [20], these corresponded to hexamers and monomers, respectively. Head & tail conformer with a variety of sizes (Figs. S1 and S2) suggests that oligomer growth may not follow an amyloid growth model [21,22] in which monomers continue attaching to seeds to form larger particles. Instead, these basic growth unit collide and coalesce to create larger oligomers [20]. These inter-oligomer interactions may be mediated by thin fibrils attached to oligomer (Fig. S2).

### Disordered conformation of $\alpha$ S monomer

HS-AFM images of  $\alpha$ S are shown in Figure 2. The conformation of  $\alpha$ S changed from almost globular (Figure 2a) to partially extended (Figure 3b), and we observed further variations in conformation [23] (data

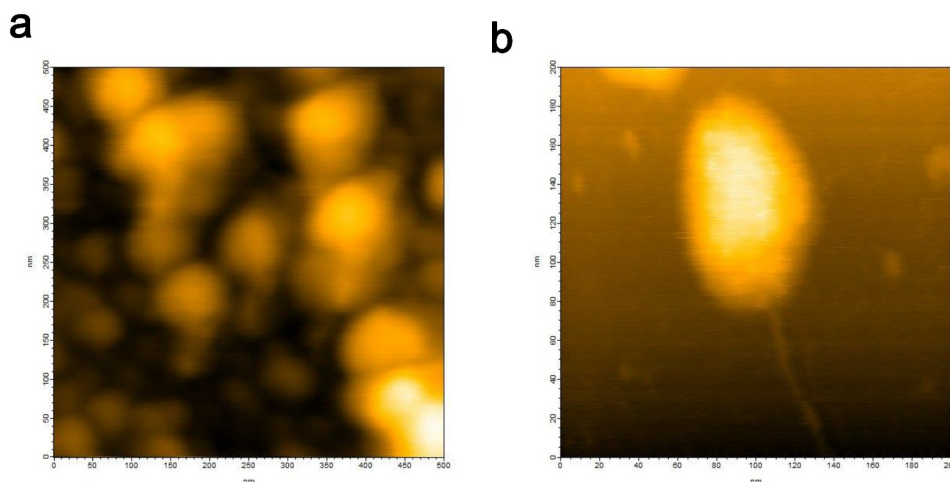


**Figure 1.** (a) HS-AFM image of hPrP showing various heterogeneous oligomeric states distributed from monomers to hexamers. (b) Typical hexameric oligomer of hPrP with a tail.

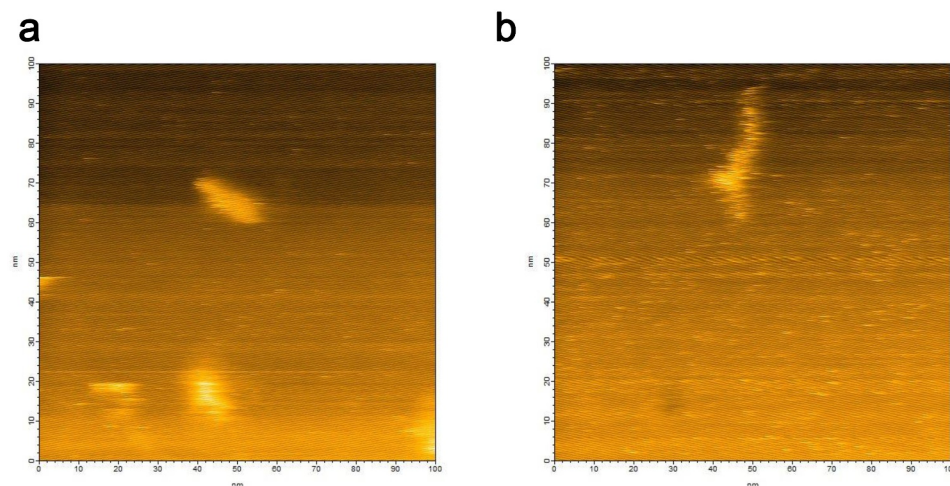


**Figure 2.** HS-AFM images of  $\alpha$ S showing (a) globular conformation and (b) extended conformation of  $\alpha$ S.

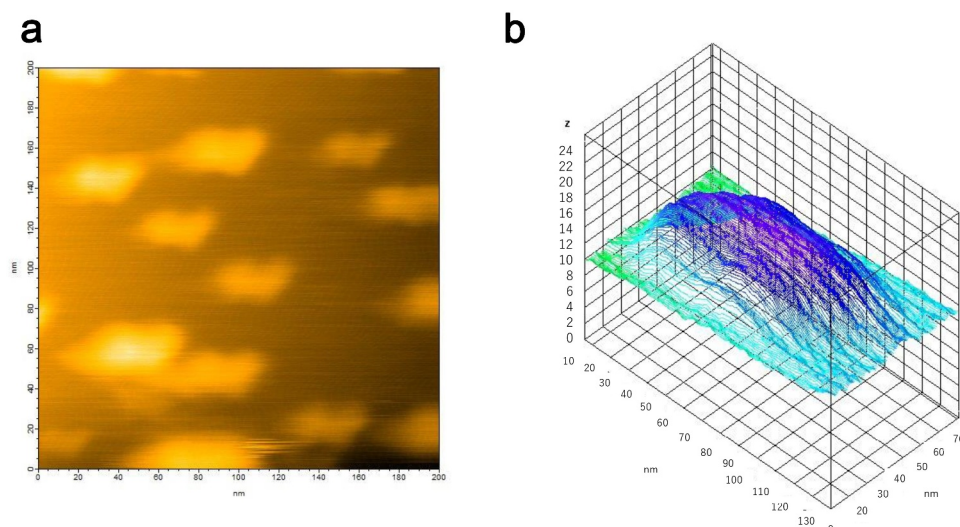


**Figure 3.** (a) HS-AFM image of hPrP and  $\alpha$ S complex at equilibrium. (b) Height analysis shows the early complex is hetero-dimer of hPrP and  $\alpha$ S. HS-AFM image of hPrP and  $\alpha$ S complex at equilibrium. Height analysis showed the oligomer at equilibrium was a trimer.

not shown). Thus,  $\alpha$ S predominantly existed as a disordered state [24,25].

### Interaction between hPrP and $\alpha$ S

The heterogeneous hPrP oligomeric configurations were confirmed after loading 1  $\mu$ l of hPrP (30 nM) onto the mica surface attached on the glass pole of the HS-AFM apparatus. Then 1  $\mu$ l of  $\alpha$ S (30 nM) was gently poured onto the mica surface. Heterogeneous oligomers of hPrP were quickly dissolved and particles with a transient shape appeared coherently within 1 frame of the HS-AFM apparatus (5 sec. in this experiment) (Fig. S3), and finally uniformly distributed dimers were shown. The height of this complex was about 2 nm (Figure 3b). In equilibrium, monomeric structure corresponding to hPrP or  $\alpha$ S, or oligomer larger than dimer was not observed. Thus this complex was considered to be hetero-dimer of hPrP and  $\alpha$ S. No further change was observed after hetero-dimer formation.

### Population shifts detected by dynamic light scattering (DLS)

While AFM is sensitive to molecular shape, it is not good at evaluating population. Therefore, DLS was used here as a complementary measurement. We initially observed that the hPrP solution was mainly populated with particles with a diameter of 24 nm (Figure 4a), suggesting that hPrP predominantly existed as oligomers. Since hPrP oligomers consist of a head and tail (Figure 1), the diffusion constant would become much slower than that of hexamer with spherical shape.

Particles with a diameter of 1.7 nm were predominantly populated in the  $\alpha$ S solution (Figure 4b). Because theoretically calculated hydrodynamic radius of  $\alpha$ S assuming spherical particle is 0.7 nm, the observed diameter indicated that  $\alpha$ S predominantly existed as a monomer. Since  $\alpha$ S is natively unfolded (Figure 2), it is reasonable that the observed diffusion constant was slower than that of spherical particle.

When hPrP and  $\alpha$ S were mixed in a one-to-one molecular ratio in solution, the oligomer peak of hPrP disappeared, and a peak at a diameter of 1.7 nm was detected (Figure 4c), which corresponds to the stable hetero-dimer of hPrP and  $\alpha$ S (Figure 3). It should be noted that this hetero-dimer were compact with no apparent tail (disordered region) (Figure 3). Thus, the diffusion constant of monomeric  $\alpha$ S and that of the compact hetero-dimer showed a close hydrodynamic radius.

### Conformational characteristics of heterodimer of hPrP and $\alpha$ S

We prepared four kinds of proteins for NMR, i.e. hPrP with or without [ $^{15}$ N] label, and  $\alpha$ S with or without [ $^{15}$ N] label. Figure 5a shows the  $^1\text{H}$ - $^{15}\text{N}$  HSQC spectra of  $^{15}\text{N}$  labelled hPrP without (blue) or with non-labelled  $\alpha$ S (red). Apparently, signals from the C-terminal half region of native hPrP were mostly disappeared and the remained peaks were broadened upon the interaction with  $\alpha$ S, suggesting the conformational conversion from native to the molten globule state. Figure 5b shows the  $^1\text{H}$ - $^{15}\text{N}$  HSQC spectra of  $^{15}\text{N}$  labelled  $\alpha$ S without (blue) or with non-labelled hPrP (red). Although native  $\alpha$ S was disordered state (IDP) [26], chemical shift of thirteen residues, i.e. L8,

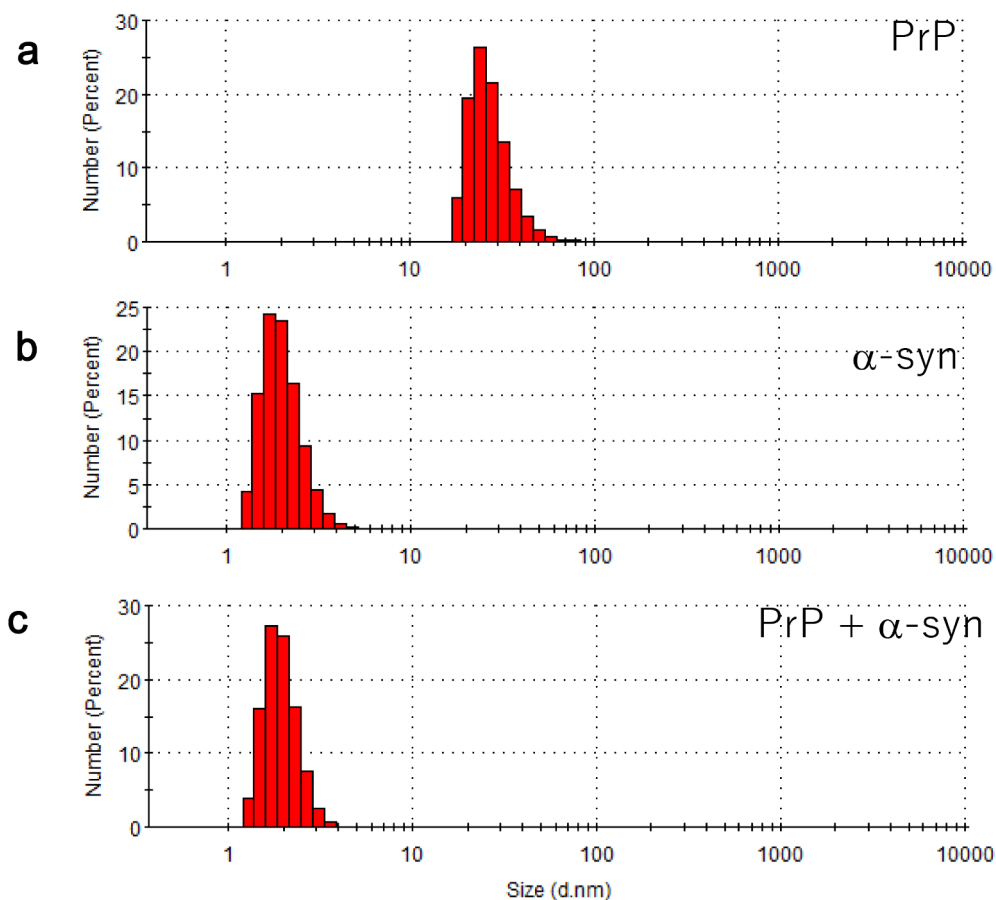


**Figure 4.** Dynamic light scattering (DLS) measurement of a number (population) of particles as a function of particle size (diameter) in (a) hPrP solution with peak at 24 nm, corresponding to an oligomer, (b)  $\alpha$ S solution with a diameter of 1.7 nm, corresponding to a monomer, and (c) a mixture of hPrP and  $\alpha$ S with a peak at the diameter of 1.7 nm corresponding to a hetero-dimer of hPrP and  $\alpha$ S.

V37, L38, V40, E83, V95, A107, Q109, D121, N122, S129, G132, and A140 were selectively shifted upon binding of hPrP, suggesting the specific contact regions in  $\alpha$ S. We plotted chemical shift alterations and the peak volume changes in  $\alpha$ S upon binding with hPrP in Fig. S4, indicating that chemical shifts in  $\alpha$ S around residues  $\sim 40$  and  $\sim 60$  were strongly perturbed (Figs. S4A & S4B), and peak intensities of C-terminal regions (residues 105  $\sim$  120) were markedly reduced (Fig. S4C).

In the present study, we found that monomer  $\alpha$ S dissolved heterogeneous hPrP oligomer into a compact dimer complex (Figure 3). This hetero-dimer of hPrP and  $\alpha$ S was rather uniform and stable, and the stable dimer formation would efficiently deplete the available monomeric hPrP molecule for pathogenic conversion [27], resulting in the suppression of misfolding of PrP and further pathogenic conformational conversion. This finding can be linked to prior research showing the chaperone-like activity of monomeric  $\alpha$ S to suppress the misfolding of a number of different proteins both *in vivo* and *in vitro* [11,28–30].

## Discussion

We previously reported that monomeric  $\alpha$ S can suppress amyloidogenesis of PrP [14], but neither bind to fully folded PrP nor fibrillar PrP [14]. Therefore we hypothesized that monomeric  $\alpha$ S binds to the hydrophobic region of partially unfolded PrP to prevent further structural changes toward misfolded aggregates [14]. This hypothesis suggests the monomer  $\alpha$ S can trap a partially unfolded (or molten globule) state of PrP which tends to oligomerize (Figure 6).

Conformation of stable hetero-dimer of hPrP and  $\alpha$ S was characterized using NMR spectra. hPrP underwent the transition from native conformation to the molten-globular state upon binding with  $\alpha$ S. In contrast in  $\alpha$ S, chemical shifts of the signals from regions including the hot spot (amino acid residue number of 38–45), amino acid residue number of  $\sim 60$  and the C-terminal region (amino acid residue number of 120–140) were selectively altered upon the interaction with hPrP, suggesting the specific interaction. Intriguingly, these regions are largely included in those involved in the

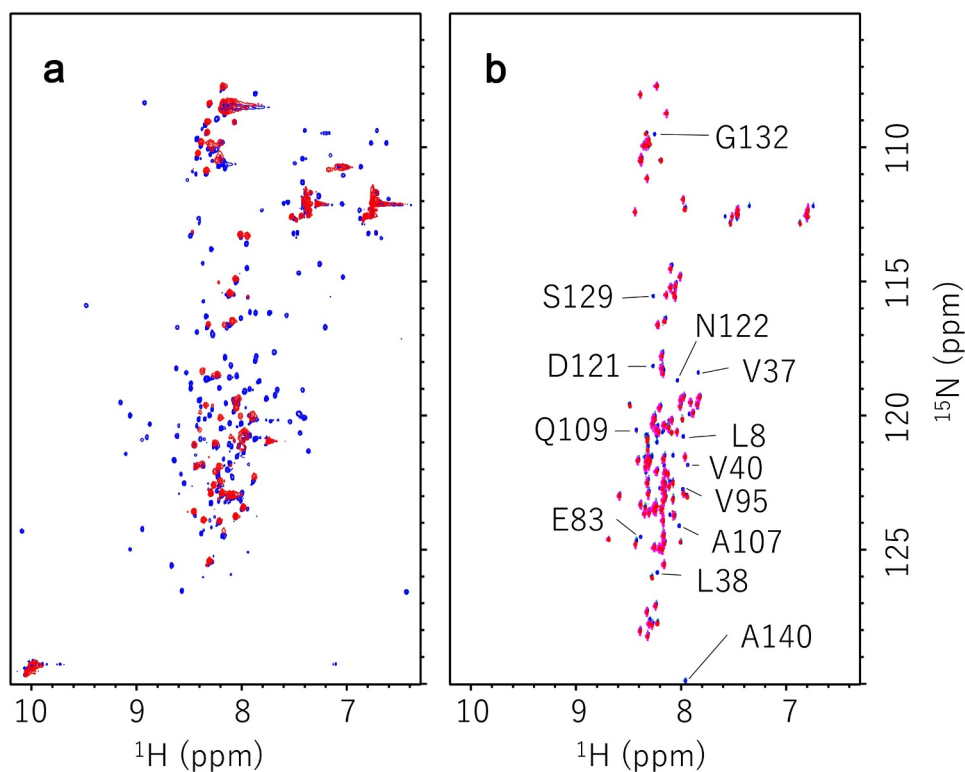


**Figure 5.** (a)  $[^1\text{H}-^{15}\text{N}]$  HSQC spectra of 200  $\mu\text{M}$   $[^{15}\text{N}]$  labelled hPrP without (blue) or with 220  $\mu\text{M}$  non-labelled  $\alpha\text{S}$  (red) at pH 6.1 in 99%  $\text{H}_2\text{O}/1\%$   $\text{D}_2\text{O}$ . (b)  $[^1\text{H}-^{15}\text{N}]$  HSQC spectra of 206  $\mu\text{M}$   $[^{15}\text{N}]$  labelled  $\alpha\text{S}$  without (blue) or with 173  $\mu\text{M}$  non-labelled hPrP (red) at pH 4.6 in 99%  $\text{H}_2\text{O}/1\%$   $\text{D}_2\text{O}$ .

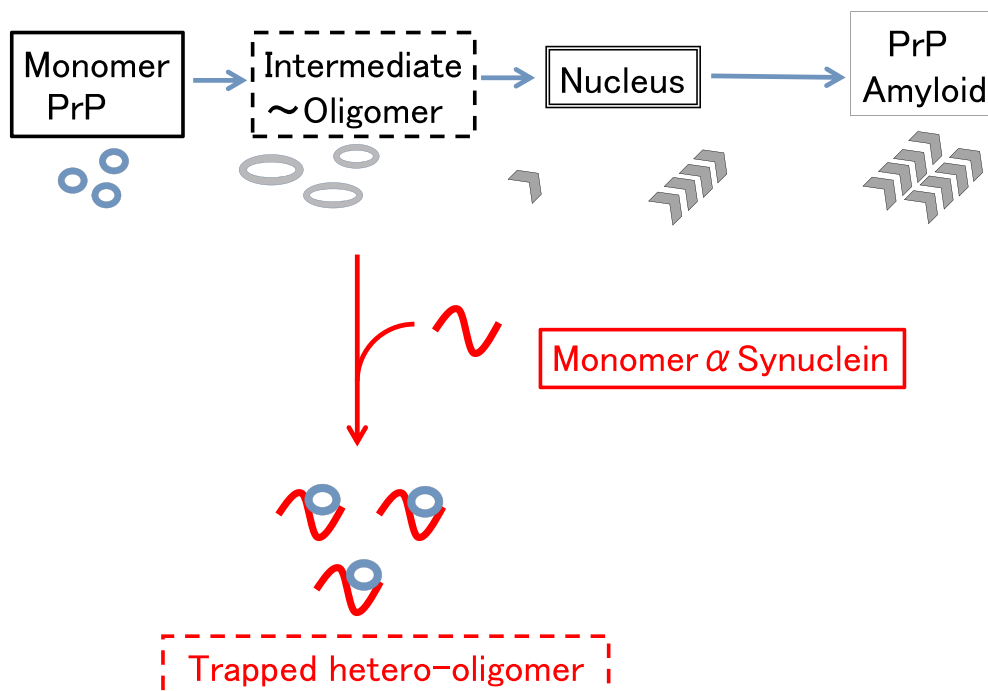


**Figure 6.** Possible mechanism of suppression of the pathogenic conversion of hPrP by  $\alpha\text{S}$ . Monomeric  $\alpha\text{S}$  can trap the intermediate state hPrP and forms a stable hetero-dimer, depleting the available monomeric hPrP for pathogenic conversion.

intermolecular interaction with  $\alpha\text{S}$  or  $\beta\text{S}$  elucidated using PRE experiments [31].

Although further studies using a kinetic methods may be required to elucidate the detailed interaction

between  $\alpha$ S and partially folded proteins [32], our results suggest a possible involvement of  $\alpha$ S in transmissible spongiform encephalopathy pathology. It was recently shown that knockout of the  $\alpha$ S gene did not affect the incubation period of prion propagation in mouse brain [33]. Since  $\alpha$ S chaperone interacts with partially folded proteins or oligomer, and suppresses the nucleation step of amyloid formation,  $\alpha$ S may suppress the spontaneous generation, or evolution [34], but not propagation of infectious prion. Although there reported the interaction between  $\alpha$ S and PrP using the immunoprecipitation and merging by immunofluorescence *in vivo* [15], there has been no corresponding *in vivo* results showing the selective inhibition of nucleation step thus far.

## Materials and methods

A plasmid encoding human PrP, amino acid residues 23–230 [hPrP] was prepared according to a previously reported protocol [35]. A recombinant hPrP was expressed using an *E. coli* expression system and purified to homogeneity according to the previously published protocol [35].

A pT7-7 vector encoding wild-type human  $\alpha$ S (residues 1–140) was purchased from Addgene (code 36,046) [14]. Recombinant human  $\alpha$ S was expressed using ECOS™ competent *E. coli* BL21 (DE3) (Nippongene, code 312–06534) and purified to homogeneity according to the previously published protocol [14].

Tapping mode high-speed atomic force microscopy (HS-AFM, NanoExplorer, Research Institute of Biomolecule Metrology Co., Ltd, Tsukuba, Japan) was performed at room temperature in aqueous solution using a small cantilever (BL-AC10FS-A2, Olympus) with a spring constant  $k \approx 0.1$  N/m and resonance frequency  $f = 1.5$  MHz. hPrP and  $\alpha$ S solutions (20 mM phosphate [pH 7.0]) were introduced into a sample chamber for HS-AFM. Image sequences were processed using ImageJ software ([imagej.nih.gov/ij/](http://imagej.nih.gov/ij/)).

To observe the interaction between hPrP and  $\alpha$ S, 2  $\mu$ L of hPrP (0.1  $\mu$ M) solution was mounted onto the mica surface on the glass pole and stayed for 10 min. and mounted again. We confirmed the clear images of the dispersive hPrP conformations, and then added 2  $\mu$ L of  $\alpha$ S (0.1  $\mu$ M), and a movie was recorded with the time resolution of 1–5 s.

DLS was performed using a Zetasizer NanoS (Malvern Panalytical, Egham, Surrey, UK). 100  $\mu$ L of hPrP solution (100  $\mu$ M) and 100  $\mu$ L of  $\alpha$ S solution (100  $\mu$ M) were used for characterizing the population in each solution. For observing the interaction between hPrP and  $\alpha$ S, we mixed

50  $\mu$ L of hPrP solution (100  $\mu$ M) and the same volume of  $\alpha$ S solution (100  $\mu$ M) and measured immediately.

NMR experiments were carried out using Avance 800 spectrometer (Bruker BioSpin) operating at a  $^1\text{H}$  frequency of 800.15 MHz and a  $^{15}\text{N}$  frequency of 81.08 MHz. A 5 mm  $^1\text{H}$  inverse detection cryogenic probe with triple-axis gradient coils was used for all measurements.  $^1\text{H}$ – $^{15}\text{N}$  HSQC spectra were acquired at 25°C, with 4,096 complex points covering 12,821 Hz for  $^1\text{H}$  and 256 complex points covering 2,108 Hz for  $^{15}\text{N}$ . NMR data were processed using the TopSpin NMR software package (Bruker BioSpin).

## Acknowledgments

This work was supported by grants from the Ministry of Health, Labour, and Welfare of Japan [Research on Measures for Intractable Diseases (Prion Disease and Slow Virus Infections, and Development of Low Molecular Weight Medical Chaperone Therapeutics for Prion Diseases #17ek0109075h)] and the Ministry of Education, Culture, Sports, Science, and Technology of Japan (Grants-in Aid for Scientific Research #19H03476). We also thank M. Kobayashi for providing technical help.

## Disclosure statement

No potential conflict of interest was reported by the author(s).

## ORCID

Ryo Honda  <http://orcid.org/0000-0003-3698-5975>

## References

- [1] Chiti F, Dobson CM. Protein misfolding, functional amyloid, and human disease. *Annu Rev Biochem.* 2006;75(1):333–366.
- [2] Legname G, Baskakov IV, Nguyen HO, et al. Synthetic mammalian prions. *Science.* 2004;305(5684):673–676. .
- [3] Riek R, Guntert P, Dobeli H, et al. NMR studies in aqueous solution fail to identify significant conformational differences between the monomeric forms of two Alzheimer peptides with widely different plaque-competence, A beta(1-40)(ox) and A beta(1-42)(ox). *Eur J Biochem.* 2001;268:5930–5936.
- [4] Shtilerman MD, Ding TT, Lansbury PT, Jr. Molecular crowding accelerates fibrillization of alpha-synuclein: could an increase in the cytoplasmic protein concentration induce Parkinson's disease? *Biochemistry-US.* 2002;41:3855–3860.
- [5] Prusiner SB. Molecular biology of prion diseases. *Science.* 1991;252:1515–1522.
- [6] Morales R, Moreno-Gonzalez I, Soto C. Cross-seeding of misfolded proteins: implications for etiology and pathogenesis of protein misfolding diseases. *PLoS Pathog.* 2013;9:e1003537.

- [7] O’Nuallain B, Williams AD, Westermarck P, et al. Seeding specificity in amyloid growth induced by heterologous fibrils. *J Biol Chem.* 2004;279:17490–17499.
- [8] Lauren J, Gimbel DA, Nygaard HB, et al. Cellular prion protein mediates impairment of synaptic plasticity by amyloid-beta oligomers. *Nature.* 2009;457:1128–U84.
- [9] Kessels HW, Nguyen LN, Nabavi S, et al. The prion protein as a receptor for amyloid-beta. *Nature.* 2010;466: E3–4. discussion E-5.
- [10] Kim TD, Paik SR, Yang CH, et al. Structural changes in alpha-synuclein affect its chaperone-like activity in vitro. *Protein Sci.* 2000;9(12):2489–2496.
- [11] Souza JM, Giasson BI, Lee VM, et al. Chaperone-like activity of synucleins. *FEBS Lett.* 2000;474(1):116–119.
- [12] Ahn M, Kim S, Kang M, et al. Chaperone-like activities of alpha-synuclein: alpha-synuclein assists enzyme activities of esterases. *Biochem Biophys Res Commun.* 2006;346(4):1142–1149.
- [13] Manda KM, Yedlapudi D, Korukonda S, et al. The chaperone-like activity of alpha-synuclein attenuates aggregation of its alternatively spliced isoform, 112-synuclein in vitro: plausible cross-talk between isoforms in protein aggregation. *PLoS One.* 2014;9(6):e98657.
- [14] Shirasaka M, Kuwata K, Honda R. alpha-Synuclein chaperone suppresses nucleation and amyloidogenesis of prion protein. *Biochem Biophys Res Commun.* 2020;521(1):259–264.
- [15] Aulic S, Masperone L, Narkiewicz J, et al. alpha-synuclein amyloids hijack prion protein to gain cell entry, facilitate cell-to-cell spreading and block prion replication. *Sci Rep.* 2017;7(1):10050. .
- [16] Ando T, Uchihashi T, Kodera N, et al. High-speed AFM and nano-visualization of biomolecular processes. *Pflugers Arch.* 2008;456(1):211–225. .
- [17] Kakuda K, Niwa A, Honda R, et al. A DISC1 point mutation promotes oligomerization and impairs information processing in a mouse model of schizophrenia. *J Biochem.* 2019;165(4):369–378. .
- [18] Kakuda K, Yamaguchi K-I, Kuwata K, et al. A valine-to-lysine substitution at position 210 induces structural conversion of prion protein into a  $\beta$ -sheet rich oligomer. *Biochem Biophys Res Commun.* 2018;506(1):81–86.
- [19] Streets AM, Sourigues Y, Kopito RR, et al. Simultaneous measurement of amyloid fibril formation by dynamic light scattering and fluorescence reveals complex aggregation kinetics. *PLoS One.* 2013;8(1):e54541.
- [20] Cho KR, Huang Y, Yu S, et al. A multistage pathway for human prion protein aggregation in vitro: from multimeric seeds to beta-oligomers and nonfibrillar structures. *J Am Chem Soc.* 2011;133(22):8586–8593. .
- [21] Nelson R, Sawaya MR, Balbirnie M, et al. Structure of the cross-beta spine of amyloid-like fibrils. *Nature.* 2005;435(7043):773–778. .
- [22] Knowles TP, Waudby CA, Devlin GL, et al. An analytical solution to the kinetics of breakable filament assembly. *Science.* 2009;326(5959):1533–1537. .
- [23] Zhang Y, Hashemi M, Lv Z, et al. High-speed atomic force microscopy reveals structural dynamics of alpha-synuclein monomers and dimers. *J Chem Phys.* 2018;148(12):123322. .
- [24] Fauvet B, Mbefo MK, Fares MB, et al. alpha-Synuclein in central nervous system and from erythrocytes, mammalian cells, and *Escherichia coli* exists predominantly as disordered monomer. *J Biol Chem.* 2012;287(19):15345–15364. .
- [25] Bhattacharya S, Xu L, Thompson D. Long-range regulation of partially folded amyloidogenic peptides. *Sci Rep.* 2020;10:7597.
- [26] Wu KP, Baum J. Backbone assignment and dynamics of human alpha-synuclein in viscous 2 M glucose solution. *Biomol NMR Assign.* 2011;5:43–46.
- [27] Kamatari YO, Hayano Y, Yamaguchi K, et al. Characterizing antiprion compounds based on their binding properties to prion proteins: implications as medical chaperones. *Protein Sci.* 2013;22:22–34.
- [28] Chandra S, Gallardo G, Fernandez-Chacon R, et al. Alpha-synuclein cooperates with CSPalpha in preventing neurodegeneration. *Cell.* 2005;123:383–396.
- [29] Rekas A, Adda CG, Andrew Aquilina J, et al. Interaction of the molecular chaperone alphaB-crystallin with alpha-synuclein: effects on amyloid fibril formation and chaperone activity. *J Mol Biol.* 2004;340:1167–1183.
- [30] Park SM, Jung HY, Kim TD, et al. Distinct roles of the N-terminal-binding domain and the C-terminal-solubilizing domain of alpha-synuclein, a molecular chaperone. *J Biol Chem.* 2002;277:28512–28520.
- [31] Janowska MK, Wu KP, Baum J. Unveiling transient protein-protein interactions that modulate inhibition of alpha-synuclein aggregation by beta-synuclein, a pre-synaptic protein that co-localizes with alpha-synuclein. *Sci Rep.* 2015;5:15164.
- [32] Arosio P, Michaels TC, Linse S, et al. Kinetic analysis reveals the diversity of microscopic mechanisms through which molecular chaperones suppress amyloid formation. *Nat Commun.* 2016;7:10948.
- [33] Bistaffa E, Rossi M, Cmg DL, et al. Prion efficiently replicates in alpha-synuclein knockout mice. *Mol Neurobiol.* 2019;56:7448–7457.
- [34] Hashimoto M, Ho G, Takamatsu Y, et al. Understanding Creutzfeldt-Jacob disease from a viewpoint of amyloidogenic evolvability. *Prion.* 2020;14:1–8.
- [35] Yamaguchi K, Kamatari YO, Ono F, et al. A designer molecular chaperone against transmissible spongiform encephalopathy slows disease progression in mice and macaques. *Nat Biomed Eng.* 2019;3:206–219.